

# Ultrasonic Assessment and Model Validation of Damage in Carbon-fiber Based Composites

Manuel Gonzales<sup>1</sup>, Gregory Graf<sup>2</sup>, Rodrigo Cooper<sup>3</sup>, Brett Nadler<sup>4</sup>, Thomas Claytor<sup>4</sup>, Trevor Tippetts<sup>4</sup>

<sup>1</sup>Dept. of Mechanical Engineering, The University of Texas at El Paso, El Paso, Texas 79968

<sup>2</sup> Dept. of Mechanical Engineering, Virginia Commonwealth University, Richmond, VA 23284

<sup>3</sup> Dept. of Mechanical Engineering, Texas A&M University, College Station, TX 77843

<sup>4</sup>Los Alamos National Laboratory, Los Alamos, NM 87545

## Nomenclature

$\tilde{T}$	Traction vector
$E_i$	Initial interfacial stiffness
$E$	Young's Modulus
$\nu$	Poisson's ratio
$G$	Shear Modulus
$\tilde{v}$	Normalized relative displacement
$\tilde{u}$	Displacement field
$\delta$	Critical displacement jump
$\lambda$	Damage parameter
$F(\lambda)$	Damage function
$\psi$	Ply location of damage
$\tau$	Ply Depth of Damage in Inches
$g$	Ultrasonic Time of Flight (subscript for Top, Damage, or Bottom plies)

## Abstract

Understanding the material interaction for induced damage in composites has become paramount because of the widespread use of composite materials in structural systems. This project will utilize ultrasonic testing to validate a finite element model that will predict damage propagation within a carbon composite. A pulse-echo ultrasound scan of coupons of the composite will detect any initial damage prior to being subjected to a regulated compression test that will cause the initiation of delamination or the propagation of existing delamination between plies.

## Introduction

Composite materials are quickly replacing many metallic-based materials in industry due to their exceptional mechanical properties, strength-to-weight ratio, and resistance to fracture [1]. The incorporation of these materials in vital components necessitates the understanding of their failure characteristics. Moreover, composite material behavior greatly differs from that of conventional isotropic structural materials due to interfacial characteristics of the plies and the matrix material [2]. As a consequence, damage initiation and propagation is sporadic due to these interfacial phenomena guiding the behavior of the material. For conventional (typically ferrous) metallic materials, large-scale impacts may produce surface damage which is easily detected via conventional surface testing methods such as liquid dye-penetrant, magnetic particle, or with simple visual inspection. However,

damage detection for composite materials is often difficult and is limited by the testing method. For example, low-velocity impacts such as bird strikes or tool drops can induce damage that may be undetectable through surface testing methods. This damage, if left undetected, can lead to catastrophic failure. Surface damage is more easily detected for metallic (isotropic) materials and is not easily manifested for composite materials due to redistribution of stresses within the reinforcing material [2]. Research is currently underway to quantify the effects of low-velocity impacts that may produce sub-surface matrix crazing as well as localized delamination, which can be difficult to detect [3]. Techniques such as acoustic emission sensing [1], shearography [4], ultrasonic immersion [5], and x-ray imaging have been proven effective for detection of damage. However, the high costs and the need for offline testing limit their feasibility in the field. Of the above nondestructive evaluation techniques, only x-ray imaging, acoustic emission, ultrasonic testing provide through-thickness characterization of sub-surface flaws [1]. The environmental and health concerns associated with x-ray testing and the greater effectiveness of ultrasound over acoustic emission makes ultrasonic inspection the preferred choice in characterizing the sub-surface flaws created by low-velocity impact.

Because of testing restrictions, it is desirable to develop models that can be used to predict the extent of possible damage [6-9] in a composite material. The predictions from these models can lead to more productive and localized testing for damage, which saves time, money, and may prevent catastrophic failures. Predictive modeling of damage in composite materials is of particular interest due to their mechanical behavior at interfaces and their fracture resistance mechanism. These models have the potential to predict the fracture behavior of interfaces, thus providing a reasonable estimate of the most probable damage scenario. Previous work on these damage models use standard or modified three-dimensional finite elements with linear-elastic material properties, which model quasi-static loads based on specified failure criteria [8] as a way to quantify the extent of the damage. To determine damage propagation in further analysis, the stiffness matrices of the failed elements are modified to eliminate elasticity through the in-plane or transverse direction. Extended research has been conducted in the area of cohesive zone modeling as a predictive method for separation of interfaces, which is the subject of this paper.

The current study is a validation of a cohesive zone model of a damaged Toray 300 carbon fiber - 934 epoxy matrix unidirectional prepeg composite plate, utilizing immersion coupled ultrasonic testing. This paper serves as a preliminary view of the study, showing the experimental setup, the finite element model creation, and the validation of the model without CZM elements. Modal analysis was first conducted on an impacted composite plate to verify an initial non-CZM finite element code, as well as the material properties derived for the model. Initial damage has been examined with baseline ultrasonic tests on coupons cut from the plate to characterize the extent of delamination caused by impact. These coupons were then subjected to controlled in-plane compression testing using an MTS 810 Material Testing System to induce further delamination. Initial calculations based on an Euler buckling scheme were made to determine the optimum coupon size for buckling to occur within compression machine limitations. The plates were then ultrasonically scanned to characterize the induced delamination from the test. The approximate locations of delamination zones were calculated based on time-of-flight measurements from the ultrasonic scanner as well as amplitude attenuation of incident sound waves on the material. An area of delamination was calculated using MATLAB based on the amount of attenuation observed by the ultrasonic test. The preliminary CZM, based on Tvergaard's CZM solution [6] was created in ABAQUS Standard<sup>®</sup> finite element analysis software using 3D quadratic hexahedral elements incorporating 47 cohesive zones, representing the 47 interfaces in the composite. Future work includes the analysis of the model under test conditions to predict the propagation of delamination from an initially damaged scenario. User defined elements will be created for the cohesive zones, each using ABAQUS's UEL interface to model the interface behavior. A full validation study will be conducted to show convergence of the CZM as well as the precision of its damage analysis.

## Experimental Methods

The composite specimen is a Toray 300 carbon fiber and 934 epoxy matrix unidirectional prepeg composite plate (2 ft x 2 ft x ¼ in), with 48 plies and a  $[0/\pm 45/90]_s$  lay-up sequence. A modal analysis was conducted on the composite plate as validation for the undamaged finite element model. The plate rested on four compliant air pedestals to simulate free-free boundary conditions. A test grid of 47 points was created on the surface of the plate and impacted with an instrumented modal hammer as seen in Figure 1.

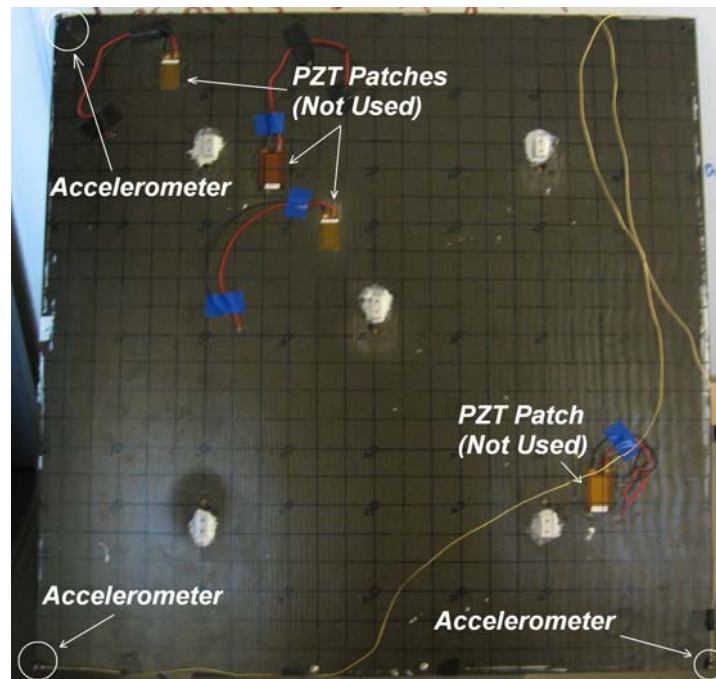


**Figure 1: Composite plate setup for modal analysis. Accelerometers were placed accordingly. PZT patches shown were used in a previous project and were removed prior to the analysis.**

Three accelerometers (Endevco® Isotron™ 2250A-10) were attached near the corners of the plate to capture the response. A LabVIEW DAQ and VI by National Instruments acquired the modal data and extracted frequency response functions (FRFs). The software, ME-SCOPE, was used to obtain the natural frequencies and characteristic mode shapes of the plate. The results from the test are shown in Table 1.

**Table 1: Modal test analysis (repeated roots denoted by asterisk)**

Experimental Frequency (Hz)	Mode Shape Description
	Torsional Mode
97	Saddle Mode
122	Umbrella Mode
170*	Second Torsional Mode
300*	Second Bending Mode

Following the modal testing, the plate was impacted with a steel projectile at various speeds and locations to generate delamination zones. A paper describing the impact testing scenario can be found in [17]. An Euler buckling analysis was performed using material properties derived from classical laminate theory [12] to determine the optimal coupon size which would permit buckling using an MTS compression loading routine. An optimal size of 2 in x 9 in x ¼ in was determined for the machine maximum load capacity of 22 kips. Material properties of the lay-up were determined for this analysis, however, more accurate values were found during the loading experiments that subsequently were used in the finite element model. The plate was cut in such a manner as to permit existing delamination in some coupons while others remained pristine.

Each coupon was then inspected using ultrasonic c-scans generated and collected with a UTEX pulser receiver. Figure 2 shows the ultrasonic scanning system with transducer, and immersion tank.

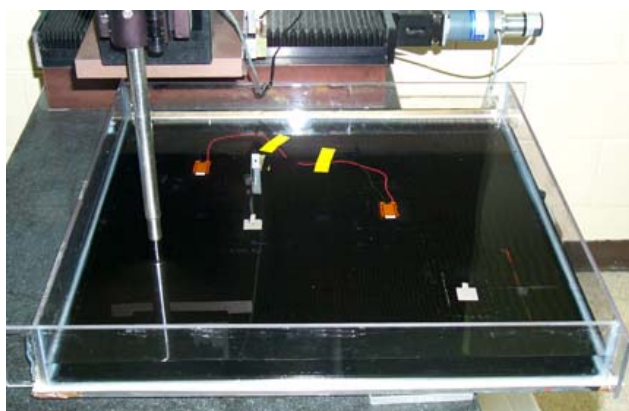


**Figure 2: Ultrasonic immersion tank with automated transducer movement before coupons**

Initial scans of the coupons were taken prior to in-plane compression testing to characterize pre-existing damage. This was accomplished using meticulous gating techniques, utilizing amplitude and time of flight attenuation techniques, to analyze the returned ultrasonic echo. Maximum amplitude gates were set for the range of front and back sound wave reflections. This ensured that only data received for front and back surface reflections was recorded. The locations and range of the gates were calculated based on the longitudinal wave speed through the material medium (using global moduli derived from laminate theory). Peaks detected at a specific time of flight were enclosed in a window, thus providing a “gate,” limiting the range of amplitude detected by the machine for front and back surface scans. Internal amplitude response gates were implemented in a similar fashion by observing amplitude peaks corresponding to areas of known damage, as well as abnormal voltage spikes in the transceiver (corresponding to obvious damage zones). Time-of-flight gates were set in conjunction with the amplitude response gates to obtain time contours of the sound wave attenuation through the material. Recording the maximum amplitude from an area in the through thickness of the plate provided a visual image of delaminated plies. Care was taken when analyzing the back surface reflection because of attenuation caused by time shifts or the shifting of the plate in the immersion tank.

After the scans, damage was grown through instrumented in-plane compression tests. The tests were conducted until changes in the load-strain curve and audible cracking occurred. Initial load-based testing resulted in catastrophic failure of coupons upon buckling. A change to displacement-rate compression prevented catastrophic buckling of greatly damaged coupons to preserve the initial geometry, while growing the internal delamination. From the 7 coupons cut from the large composite plate, 2 experienced catastrophic failure, thus preventing further meaningful ultrasonic scanning. Figure 3 shows the buckling of the composite in the test fixture.

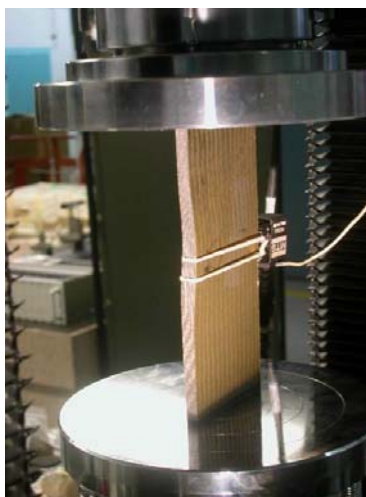


**Figure 1: Compression test setup. Extensometer is attached to the coupon as shown.**

## Computational Models

Crack propagation through a material creates interfaces which must somehow be tracked to obtain a final damage scenario. Conventional Lagrangian methods necessitate frequent re-meshing and enriching of finite elements at crack tips to properly characterize the physics of the growth. Thus, meshless methods are becoming popular in analyzing crack growth and solving interface tracking problems [10, 11]. Cohesive Zone Models (CZMs) provide damage propagation through the implementation of a traction-separation law and a corresponding energy-release rate relationship to a quadratic finite element mesh. This, in contrast to the previously stated method, allows visualization of damaged interfaces due to the traction behavior. Cohesive zone modeling provides a different perspective on characterizing failure for complex materials that are largely dominated by interfacial effects, including composite and grain boundary fracture phenomena. CZMs have been implemented in many composite material problems involving oriented and disoriented fibers to describe the constitutive behavior of the material [13–15].

In most cases, linear-elastic relationships were used as first approximation to the material behavior of the matrix and fiber. Material non-linearity as well as manufacturing defects in composites hinder the characterization of damage propagation. Thus, a failure criterion must be employed to describe the regions of failure in a composite by approximating material non-linearity as closely as possible, while incorporating any initial material defect conditions from manufacturing.

Frequently, matrix-fiber debonding occurs if the traction on the matrix-fiber interface reaches a critical level, dependent on the interfacial strength [12]. Approximations of the traction vector can typically be modeled based on CZM traction in the general form [16]:

$$\tilde{T}(\tilde{u}) = E_i \tilde{v} F(\lambda), \quad (1)$$

where the damage parameter  $\lambda$  takes on values of 0 for pristine condition materials, and 1 for complete separation of two previously joined interfaces. The vector  $\tilde{v}$  is defined as the normalized relative displacement vector of the cohesive elements, given by:

$$\tilde{v} = \frac{\tilde{u}}{\delta}, \quad (2)$$

where now the critical jump in displacement across the interface,  $\delta$ , is defined. More information on critical solution jumps and their importance to CZM is given by Chaboché et al [9]. In a simplified form, the damage function takes the following meaning [6, 16]:

$$F(\lambda) = \begin{cases} (1-\lambda)^2 & \lambda \leq 1 \\ 0 & \lambda > 1 \end{cases}. \quad (3)$$

As stated by Tippetts et al [16], the function is equivalent to the CZM originally used by Tvergaard [6] for mode I fractures. Shown in Figure 4 is a typical traction-separation CZM curve.

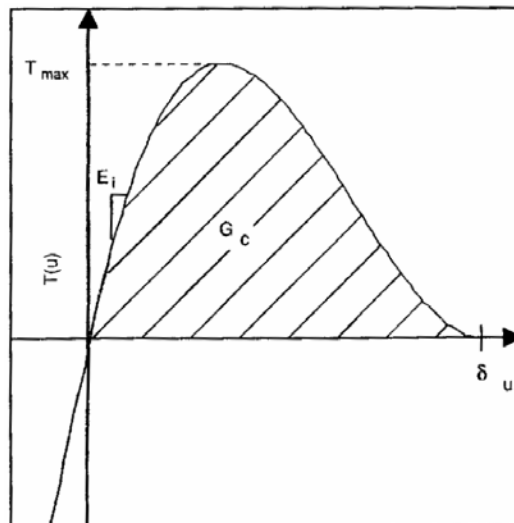


**Figure 2: Typical CZM Traction-Separation curve (Adapted from [16])**

An initial 3D model was created in ABAQUS Standard<sup>®</sup> finite element software representing the coupon geometry. Sections were partitioned to represent the ply lay-up of the material. As a result, 48 layers were created, each with the specific material properties in the lay-up orientation previously described. Each partition boundary for the layers was re-partitioned to cover 5% of two adjacent layers, thus creating a very thin interfacial layer representation. The coupons were meshed using 3D hexahedral elements with a total of 9216 elements. Each partitioned layer had one element in the through-thickness, thus creating 47 instances (referring to the thin interfaces created) where elements had an aspect ratio greater than 100 to 1. Figure 3 shows the through-thickness view of the finite element model. Boundary conditions and degrees of freedom simulated those of the controlled in-plane compression test. Ply orientations were accounted for using ABAQUS's built-in property orientation function (which simulates the use of the transformation matrix). Preliminary finite element analysis was conducted on pristine condition models (models containing no damage) to verify the validity of boundary conditions, using quasi-static load conditions with a load ramp function.

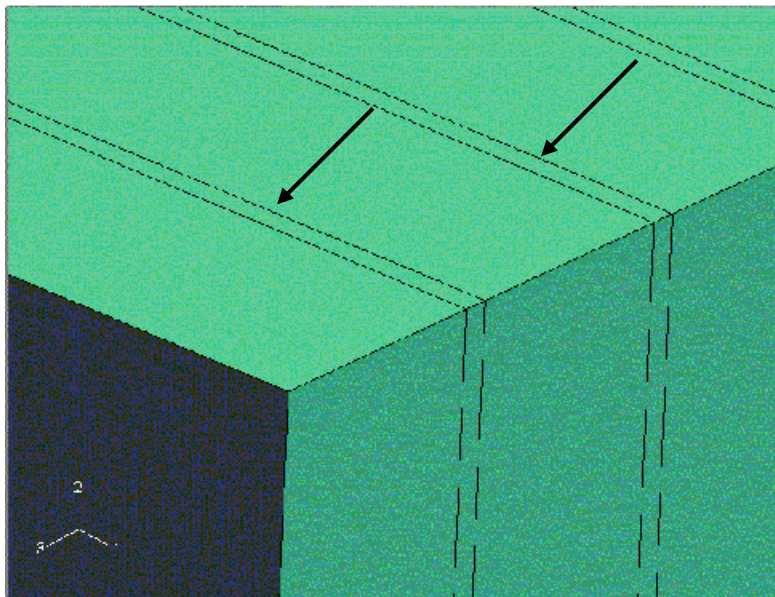


**Figure 5: Close-up of coupon CZM. Arrows denote the cohesive zones.**

Modal analysis data from Table 1 was compared with the finite element model using both plate and 3D hexahedral elements. Table 1 shows a summary of the first six natural frequencies and mode shapes for both plate and hexahedral elements. The hexahedral element mesh shows a greater deviation from the experimental frequency due to the insufficient refinement through the thickness to accurately model the stress fields induced by plate bending. Also, the analysis was done using a pristine model, in contrast with the experimental frequency, which was obtained from a damaged plate. However, the frequencies obtained are within an acceptable error range, and thus the material properties used are within reasonable bounds.

**Table 2: Experimental and FE modal test summary (repeated roots denoted by asterisk)**

Experimental Frequency (Hz)	Plate Element Frequency (Hz)	Hex. Element Frequency (Hz)	Error for Plate Elements	Error for Hex. Elements	Mode Shape Description
66.4	67.3	60.9	1.31%	8.30%	Torsional Mode
97	98.4	93.9	1.41%	3.23%	Saddle Mode
122	123.3	118.5	1.09%	2.88%	Umbrella Mode
170*	174.3	165.4	2.55%	3.28%	Second Torsional Mode
300*	309.1	277.1	1.95%	7.64%	Second Bending Mode

## Results and Discussion

The internal amplitude response, back amplitude response, and internal time-of-flight response prior to compression testing for coupon 4 are shown in figures 6 – 4. The delamination areas serve as an initial starting point in characterizing the deformation behavior of composites.

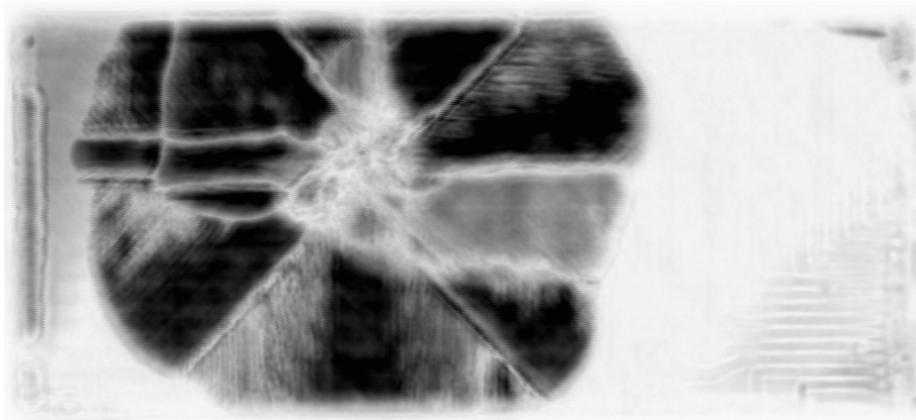


**Figure 6: Internal amplitude response of a damaged coupon**

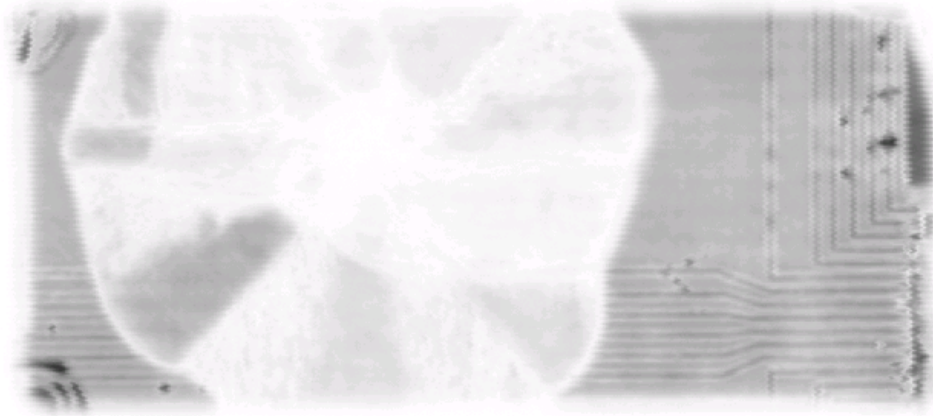


**Figure 7: Back reflection amplitude response showing attenuation due to delamination**

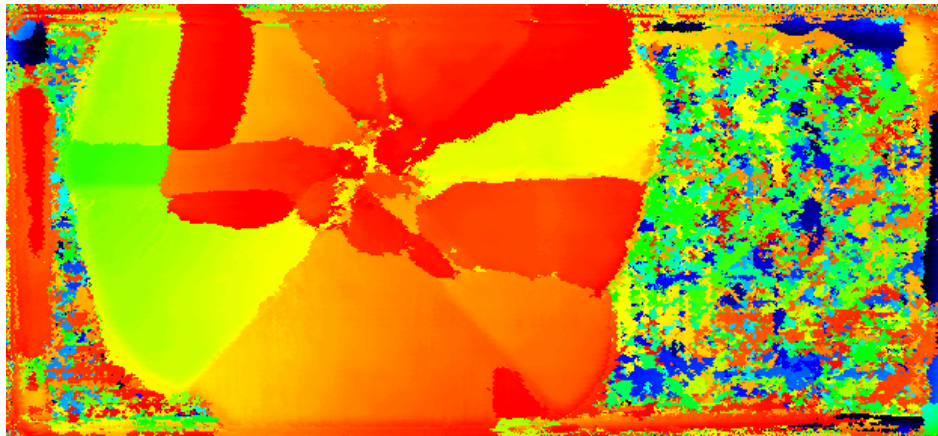


**Figure 8: Internal time response showing various delaminations**

The approximate delamination locations were determined through a ratio of flight times multiplied by the number of plies or total thickness of the plate. This gives an approximation of the damage location to within two or three plies. Equation 4 has a factor relating to the total number of plies, 48, while equation 5 relates to the plate thickness.

$$\psi = \frac{\mathcal{G}_d - \mathcal{G}_t}{\mathcal{G}_b - \mathcal{G}_t} \times 48 \quad (4)$$

$$\tau = \frac{\mathcal{G}_d - \mathcal{G}_t}{\mathcal{G}_b - \mathcal{G}_t} \times 0.25 \quad (5)$$

An approximation of the delamination area at several depths is obtained by calculating scanning resolution over the internal time response contours for the respective ply separations.

Each ultrasound image was imported into MATLAB and subsequently decoded, changing pixels to elements of a coordinate matrix. Each pixel is assigned a numerical value, corresponding to the amplitude response or time-of-flight. Estimates of the delamination area can be obtained by evaluating the amount of signal attenuation difference from pre and post compression scans. The area of delamination is calculated by determining the amount of points (pixels) falling into a specific time-of-flight range, and comparing them to the total amount of points in the image. Table 3 presents the delamination growth of the coupons and the maximum compressive load applied for each compression test. Damage for coupons 1 and 7 was so severe that meaningful scanning post-compression would not be feasible, and thus the data was omitted.

**Table 3: Average delamination growth and maximum compressive load for each coupon**

Coupon	Avg. % Delam. Pre-compression	Avg. % Delam. Post compression	Percent Delamination Growth	Maximum Loading (kips)
2	5.0	6.1	1.1	17.6
3	7.9	29.2	21.3	20.1
4	52.0	53.3	1.3	---
5	4.2	89.3	85.1	19.8
6	4.4	8.0	3.4	14.5

Preliminary finite element calculations on a pristine coupon showed a strong correlation between the measured strains during testing and the calculated strains from the model. Deviations of the strain values increased as the amount of delamination present in the coupons increased.

### Summary and Future Work

Due to their outstanding mechanical properties and low density, composite materials are readily being incorporated in crucial machine components. However, their fracture behavior is sporadic and thus structural health monitoring and field NDE methods are of paramount importance to the well-being of the component. Accurate finite element models of anisotropic composite materials provide a reasonable prediction of the fracture behavior of these materials. Various methods currently exist to describe the behavior of the material under load, as well as describe the failure characteristics of the material. A cohesive zone model was created using ABAQUS to model a 48 ply Toray 300 carbon fiber – 934 epoxy matrix coupon under in-plane compression loading. Ultrasonic scanning characterized the extent of impact damage on coupons and the delamination area was determined using MATLAB<sup>®</sup>. Controlled in-plane compression testing was conducted to further propagate any present damage or nucleate damage in the composite. Ultrasonic scanning was again performed to obtain an estimate of delamination growth and localized damage area. This paper serves as a preliminary report on the work being done at Los Alamos National Laboratory. Work is underway to implement user defined elements in the ABAQUS algorithm by differentiating cohesive elements from fiber elements using a reduced integration marker. The UEL user interface will be used to change the definition of the elements. Initial damage to the plates was characterized by baseline ultrasonic scanning, as previously stated. The next step in the process involves reproducing the areas of delamination of the various coupons in ABAQUS by displacing elements or completely removing them. A quasi-static compression will simulate the propagation of damage from the initial damage scenario with the incorporation of the cohesive law for the CZM elements. A validation procedure will be implemented after evaluating finite element models for each coupon comparing delamination areas to the computationally predicted damage scenarios.

### Acknowledgements

The authors would like to thank their mentors, Brett Nadler and Thomas Claytor, for their tireless assistance and providing subject matter knowledge. This research was funded through the Los Alamos National Laboratory Dynamics Summer School under the tutelage of Dr. Charles Farrar.

### References

- [1] McMullen, P. *Fibre/resin composites for aircraft primary structures: a short history, 1936-1984*. Composites 15(N3). 222-230. 1984.
- [2] Meyers, MA. *Mechanical Behavior of Materials*. Prentice Hall. 637 – 665. 1999.
- [3] Kaczmarek H, Maison S. *Comparative Ultrasonic Analysis of Damage in CFRP Under Static Indentation and Low-Velocity Impact*. Composites Science and Technology 51. 11 – 26. 1994
- [4] Favre JP, Laizet JC. *Amplitude and Counts per Event Analysis of the Acoustic Emission Generated by the Transverse Cracking of Cross-ply CFRP*. Composites Science and Technology Issue 36: 27-43. 1989.

- [5] Okafor AC, Otieno AW, Dutta A, and Rao VS. *Detection and Characterization of High-velocity Impact Damage in Advanced Composite Plates Using Multi-sensing Techniques*. Composite Structures Issue 54: 289-297. 2001.
- [6] Tvergaard, V. Effect of Fibre Debonding in a Whisker-reinforced Metal. *Materials Science and Engineering*, (A125). 203 – 213. 1990.
- [7] Niordson CF, Tvergaard V. *Nonlocal Plasticity Effects on Fibre Debonding in a Whisker-Reinforced Metal*. *European Journal of Mechanics A/Solids* 21. 239 – 248. 2002.
- [8] Freitas M, Silva A, Reis L. *Numerical Evaluation of Failure Mechanisms on Composite Specimens Subjected to Impact Loading*. *Composites: Part B* 31. 199 – 207. 2000.
- [9] Chaboche JL, Feyel F, Monerie Y. *Interface Debonding Models: A Viscous Regularization with a Limited Rate Dependency*. *International Journal of Solids and Structures* 38. 3127 – 3160. 2001.
- [9] Aymerich F, Meili S. *Ultrasonic Evaluation of Matrix Damage in Impacted Composite Laminates*. *Composites: Part B* 31. 1 – 6. 2000.
- [10] Belytschko T, Black T. *Elastic Crack Growth in Finite Elements with Minimal Remeshing*. *International Journal for Numerical Methods in Engineering* 45. 601 – 620. 1999.
- [11] Ventura G, Xu JX, Belytschko T. A Vector Level-Set Method and New Discontinuity Approximations for Crack Growth by EFG. *International Journal for Numerical Methods in Engineering* 54. 923 – 944. 2002.
- [12] Berthelot JM. Composite Materials: Mechanical Behavior and Structural Analysis. Springer-Verlag. 1999.
- [13] Li S, Thouless MD, Waas AM, Schroeder JA, Zavattieri PD. Use of Mode-I Cohesive-Zone Models to Describe the Fracture of an Adhesively-Bonded Polymer-Matrix Composite. *Composites Science Technology* 35. 281-293. 2005.
- [14] Dwivedi SK, Espinosa HD. *Modeling Dynamic Crack Propagation in Fiber Reinforced Composites Including Frictional Effects*. *Mechanics of Materials* 35. 481 – 509. 2003.
- [15] de Moura MFSF, Gonçalves JPM. *Modeling the Interaction Between Matrix Cracking and Delamination in Carbon-Epoxy Laminates Under Low Velocity Impact*. *Composites Science and Technology* 64. 1021 – 1027. 2004.
- [16] Tippetts T, Hemez FM, Williams TO. *Damage Prognosis Solutions, Part II: Validation*. Los Alamos National Laboratory Report. LA-UR-05-0572.
- [17] Wait JR, Ellis R, Park G, Sohn H, Hunter NF, Salazar I, Nadler B, Farrar C. *Sacrificial Composite Plate Impact Test Results*. Testing Report. Damage Prognosis LDRD-DR group. ESA-WR Division. Los Alamos National Laboratory. 2003.